Mineralogical Magazine, August 1999, Vol. 63(4), pp. 535–558

The granitic pegmatites of the Fregeneda area (Salamanca, Spain): characteristics and petrogenesis

E. RODA ROBLES[1], A. PESQUERA PEREZ[1], F. VELASCO ROLDAN[1] AND F. FONTAN[2]

[1] Departamento de Mineralogía y Petrología, Universidad del País Vasco 644, E-48080, Bilbao, Spain
[2] Laboratoire de Minéralogie, Université Paul Sabatier, F-31000 Toulouse, France

ABSTRACT

Pegmatites of the Fregeneda area, Salamanca, Spain, show a zonal distribution, from barren to enrichment in Li, Sn, Rb, Nb>Ta, B and P. They intrude pre-Ordovician metasediments which were metamorphosed to sillimanite-zone conditions near the Lumbrales granite. Field, mineralogical and petrographic data show the following zonal sequence from the granite outward: (1) barren pegmatites (pegmatites T1, T2, T3 and T4) with quartz, K-feldspar > albite, muscovite, tourmaline ± andalusite ± garnet; (2) intermediate pegmatites (types T5 and T6), characterized by the occurrence of beryl and Fe-Mn-Li phosphates; and (3) fertile pegmatites (dykes T7 and T8), with lepidolite, cassiterite, columbite, albite > K-feldspar, montebrasite and spodumene.

Tourmaline from different pegmatites shows significant compositional variations. Trace element variations in mica and K-feldspar suggest that the origin of the different pegmatitic bodies may be explained by three different paths of fractional crystallization of melts generated by partial melting of quartzo-feldspathic rocks.

KEYWORDS: granitic pegmatites, mineralogy, trace element modelling, petrogenesis.

Introduction

GRANITIC pegmatites occur in spatially and/or genetically definable groups and it is known that different types of pegmatite show a zonation around a granitic intrusion. Close to the granites, barren pegmatites appear, whereas the more evolved forms occur furthest from the batholith. Generally, the degree of evolution is not only noticed in the mineralogy of pegmatite, but also in the chemical composition of minerals, as well as in the internal structure of the pegmatite body. Thus, the more evolved pegmatites are enriched in lithophile rare elements (Li, Rb, Cs, Sn, Nb, Ta, Be, P, F, B). This enrichment allows for the occurrence of some unusual minerals such as lepidolite, spodumene, amblygonite, petalite, elbaite, Fe-Mn phosphates, columbite and beryl, etc.

Minerals in pegmatites have often been used as geochemical indicators, as well as to estimate the economic potential of these rocks (Shmakin, 1979; Shearer *et al.*, 1985, 1992; Černý, 1992; Neiva, 1995; Mulja *et al.*, 1995; Kontak and Martin, 1997; Lottermoser and Lu, 1997). In order to evaluate the character of the source rock, the petrogenetic link between the different pegmatite types, and between the parental granite and the pegmatites, several processes are considered. One of the most widely accepted models involves the fractionation of granitic magmas according to the model of Jahns and Burham (1969), who emphasized the role of H_2O and other volatile elements in the evolution of pegmatitic bodies. However, London (1992) suggested that the saturation in an aqueous phase is not necessary for the formation of pegmatitic textures. Partial melting of a metasedimentary rock may be another possible process which produces the wide compositional variation observed in some pegmatite fields. In any case, we have to consider the possibility of a combination of different degrees of partial melting and fractional crystallization.

In this paper, the pegmatite field of the Fregeneda area (Salamanca, Spain) has been

studied. Different types of pegmatite have been defined according to their mineralogy, morphology and internal structure. A mineralogical and geochemical approach is suggested to understand the main features of this pegmatite field. The model has been created by studying several samples from the different pegmatite types recognized in this area. Thus, the possible petrogenetic processes that produced the Fregeneda pegmatites and the associated granites, as well as the relations among the different pegmatite types, and among the pegmatites and the granites of the area are evaluated.

Regional geology

Deformation and metamorphism

The Fregeneda area is in the Hesperic Massif, in the western part of a narrow metamorphic belt, with an E–W trend. This belt, situated in northwestern Salamanca, is bordered by the Lumbrales granite to the South, and by the Saucelle granite to the NE (Fig. 1). Both granites and pegmatites intruded pre-Ordovician metasediments of the schist-metagreywacke complex. In this area, this complex comprises a sequence of quartzites, greywackes, schists and pelites, with abundant thin calc-silicate layers. These materials have undergone two main phases of Hercynian deformation, with late events of less intensity (Martínez Fernández, 1974). The earliest phase produced a foliation plunging N with a NW–SE strike, and parallel to the axial plane of isoclinal folds. This gave rise to an important set of fractures, striking N30°E and dipping $80 \pm 10°$ to the East. The second phase produced a crenulation over the previous schistosity, a lineation of the blastic biotites and the boudinage of some levels (López Plaza *et al.*, 1982). Likewise, the deformation of the Lumbrales granite is attributed to this phase of deformation, as well as to a set of fractures striking N10°E and dipping $75 \pm 5°$ to the East. Finally, a late deformation process has been recognized, which produced wide folds, kink-bands, and NE-SW fractures, some carrying quartz segregations known locally as 'sierros' (García de Figuerola and Parga, 1971).

The regional metamorphism occurred prior to the second phase of Hercynian deformation (Carnicero, 1982), and a contact metamorphism is superimposed on it. This may be due to the presence of a hidden granitic body, which has been detected at depth by drillings (López Plaza *et al.*, 1982). In the Fregeneda area, the metamorphism shows an isograd distribution parallel to the Lumbrales granite, reaching the sillimanite zone locally, whereas the biotite zone is the most extensive (Fig. 1).

Igneous rocks

A great diversity of granites crop out in the Fregeneda area. The most common group is that of the peraluminous leucogranites, to which the Lumbrales and the Saucelle granites belong (Fig. 1). Both are parautochthonous, heterogeneous, fine- to medium-grained two-mica granites (Carnicero, 1981) and are included in the group of syntectonic massifs which have been affected by the third phase of Hercynian deformation (López Plaza and Carnicero, 1988; López Plaza and Martínez Catalán, 1988). The Lumbrales granite is part of the Meda-Penedono-Lumbrales granitic complex (Bea *et al.*, 1988), with a Rb-Sr whole-rock isochron age of 300 ± 8 m.y. (García Garzón and Locutura, 1981). In spite of its evident petrological continuity, the Lumbrales granite shows a clear tectonic control westwards, whereas to the east the deformation decreases and the emplacement of the granite is free of external stress (Gonzalo Corral, 1981; López Plaza *et al.*, 1982). Another characteristic of this body is the presence of a migmatitic facies in the border as well as in the inner zones. This facies typically has a layered structure, occasionally folded (Mata Burillo, 1986) and mainly occurs to the east of the Fregeneda area.

Finally, a group of calc-alkaline post-tectonic granites is also important in the area, e.g. the late-Hercynian, calc-alkaline Villar del Ciervo granite, which crops out to the south of the Lumbrales granite (Fig. 1) and with a Rb-Sr whole-rock isochron age of 284 ± 8 m.y. (García Garzón and Locutura, 1981). Li-bearing pegmatites of similar characteristics to those of the Fregeneda area also occur associated with the Villar de Ciervo granite.

General geology of pegmatites

In the Fregeneda area, approximately 800 pegmatitic bodies have been found. On the grounds of factors such as mineralogy, morphology, internal structure, and internal relationships, eight different types of pegmatites have been distinguished. These different types display a degree of evolution which increases away from the Lumbrales granite. With increasing distance from this granite the types are as listed

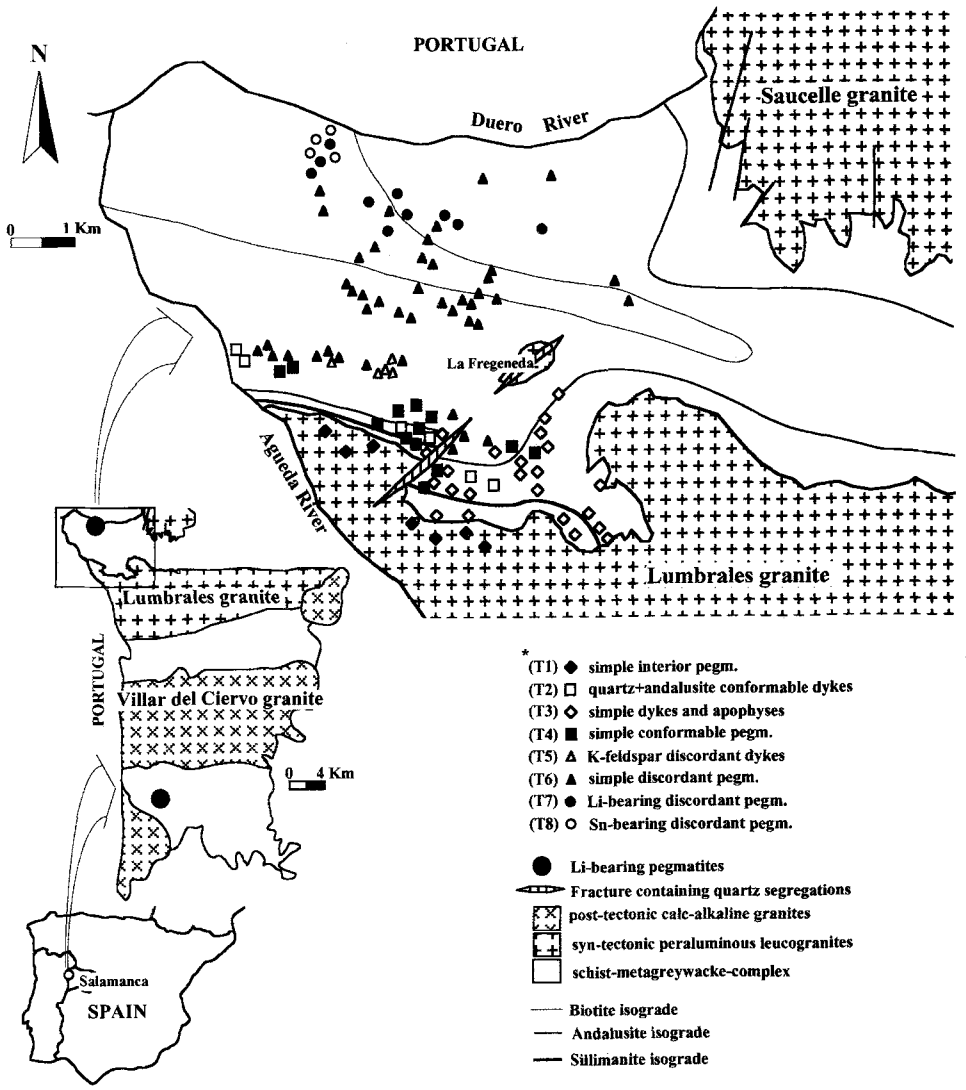

FIG. 1. Geological map of the study area and distribution of the pegmatite groups recognized. (* pegmatite numbers as in Table 2).

below (Roda, 1993; Roda *et al.*, 1995*a,b*, 1996), (Fig. 1, Tables 1, 2).

Intragranitic pegmatites (TI)

These are relatively abundant in the border zones of the Lumbrales granite. They consist of quartz, K-feldspar (orthoclase and microcline), muscovite, albite and schorl. In addition, very altered heterosite may be present as an accessory mineral, mainly to the west of the area. These pegmatite dykes are narrow, and they are oriented oblique to the granite lineation. Frequently, these pegmatites show a zoned internal structure (Fig. 2*a*), with a core of massive quartz and a border zone consisting of coarse-grained K-feldspar, albite and tourmaline.

TABLE 1. Main characteristics of the groups of pegmatites recognized in the Fregeneda district

Type	Mineralogy		Nature of the host rock		Morphology and structure	% of the total pegmatitic volume	Outcrop area	Remarks	Enrichments
	Main minerals	Other important minerals	Tourmal-inization	Country rock					
T1	Qtz Ksp	msc ab tur	–	(intragranitic)	dyke-like thickness <50 cm	~2%	within the Lumbrales *granite*	within the Lumbrales granite	K, Al, Si, (B, P)
T2	Qtz and	msc tur Ksp chl	–	Andalusite zone	conformable dyke-like thickness <40 cm	~4%	close to the Lumbrales granite	boudinage structures. Dykes mainly of qtz and andalusite	Al, Si, (B, K)
T3	Qtz Ksp msc	ab tur bi	–	Sillimanite, andalusite and biotite zones	irregular and bulbous masses ellipsoidal, lenticular or turnip-shaped	~10%	S-E of the area near the Lumbrales granite	abundant; aplite-pegmatite facies; graphic texture	K, Al, Si, (B)
T4	Qtz Ksp msc ab tur	and chl gt bi	V	Sillimanite and andalusite zones	forms conformable dyke-like locally with internal zonation thickness of 1 m	~20%	near the Lumbrales granite	abundant; in some cases internal zoning, and graphic texture	B, Al, Na
T5	Ksp	Qtz msc pyrite	–	Biotite zone	disconformable dyke-like thickness >1 m	<4%	1 km from the Lumbrales granite	not very abundant; main component is pink K-feldspar	K
T6	Qtz Ksp ab msc	±Fe-Mn pho ±amb ±tur	V	Biotite and chlorite zones	disconformable dyke-like thickness <10–200 cm	~50%	1–4 km from the Lumbrales granite present	most abundant Near the Lumbrales granite, internal zoning can be	K, Na, Al, Si, (P, Li)
T7	Qtz ab Li-mica msc Ksp	amb spd cass apt	V	Biotite and chlorite zones	disconformable dyke-like sometimes with internal zoning thickness <1–15 m	~8%	not very abundant; 4–6 km from the Lumbrales granite	can show internal zonation. Li-bearing minerals are very abundant	Li, Sn, P, (Rb, Cs)
T8	Qtz cass ab	msc Ksp	V	Chlorite zone	disconformable dyke-like, thickness < 50 cm locally with internal zoning	~2%	N of the studied area	rare, folded with a reduction in the height. Cassiterite.	Sn, K, (P)

Qtz – quartz; Ksp – K-feldspar; msc – muscovite; ab – albite; tur – tourmaline; and – andalusite; chl – chlorite; bi – biotite; gt – garnet; py – pyrite; pho – phosphates; amb – amblygonite; spd – spodumene; cass – cassiterite; apt – apatite; be – beryl.

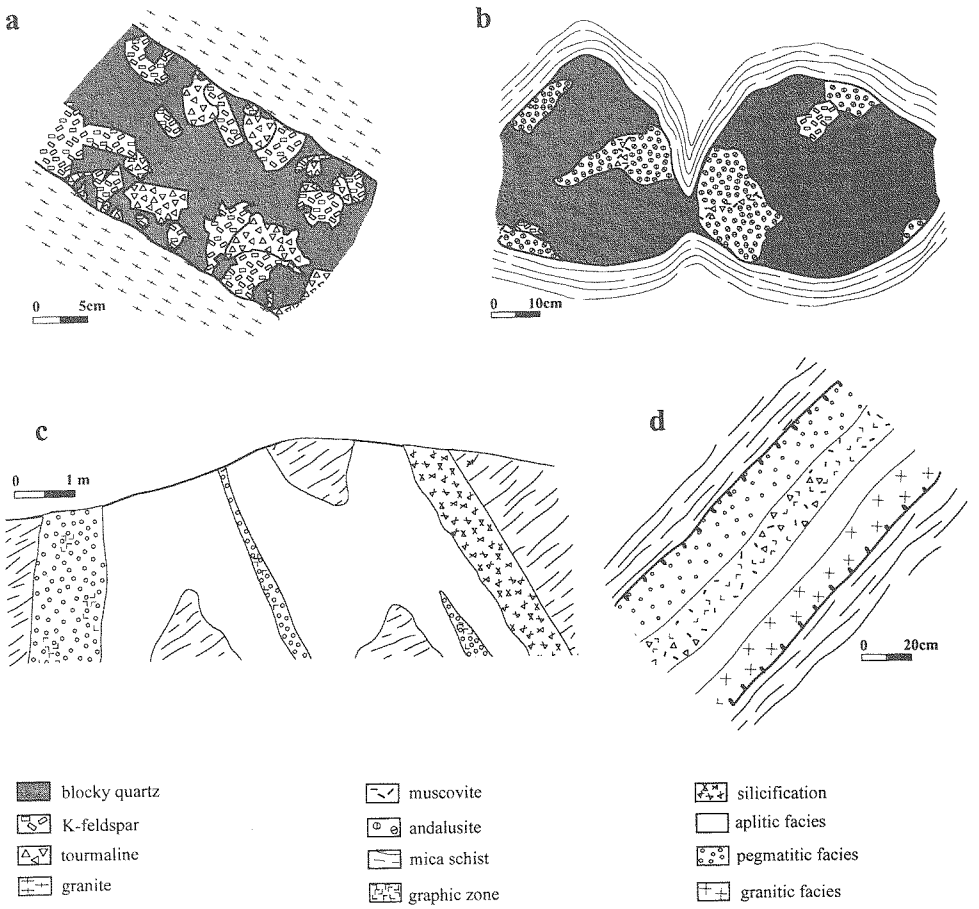

FIG. 2. Schematic section of the internal structure showed by the barren pegmatites and dykes: (*a*) intragranitic T1 pegmatites; (*b*) quartz-andalusite T2 dykes; (*c*) apophyses with aplitic and pegmatitic facies (T3); and (*d*) simple conformable T4 pegmatites.

Dykes composed mainly of quartz and andalusite (T2)

They include sparse muscovite, K-feldspar (orthoclase and microcline), schorl and chlorite. They show an E–W strike, and different dipping. These dykes conform to their host-rocks, showing an appropriate deformation with boudinage structures (Fig. 2*b*).

Dykes and apophyses showing aplitic and pegmatitic facies (T3)

These consist of quartz, K-feldspar (orthoclase and microcline), muscovite and minor albite, biotite and schorl. Graphic textures occur locally in these bodies. Their shapes are greatly variable, ranging from irregular and bulbous masses to ellipsoidal, lens-like or turnip-shaped forms. Their size also varies, from a few square metres up to 1 km^2. The grain size varies abruptly within centimetres from aplitic to pegmatitic facies. Some of these bodies exhibit a silicified tectonic contact with the enclosing rocks (Fig. 2*c*). They are located SE of the studied area, near the Lumbrales granite.

Simple conformable pegmatites (T4)

These are mainly composed of quartz, K-feldspar (orthoclase and microcline), muscovite, albite,

TABLE 2. Petrographic characteristics of the different phases associated with the different pegmatite types of the Fregeneda area. (*Pegmatite types numbered as in Fig. 1)

	Petrographic type	Shape and habit	Grain size	Textures and microstructures	Distribution *Pegmatite types							
					1	2	3	4	5	6	7	8
Quartz	I	sub- to anhedral	fine to coarse	undulatory extinction, deformation bands and lamellae, subgrains	■	■	■	■	■	■	■	■
	II	vermicular to cuniform	fine to medium	granophyric or graphic intergrowths, with Ksp	■		■	■		■	■	
	III	vermicular, flamee, or blebs	<200 μm	myrmekitic intergrowths						■	■	
	IV	anhedral, lens-like	fine	intergranular			■					
	V	polygonal	very fine	granoblastic texture, asssociated with deformation bands and grain limits	■		■	■	■	■	■	
	VI	subhedral to anhedral	very fine to fine	microfaracture filling			■	■			■	
K-spar	I	euhedral to anhedral	fine to coarse	cross-hatch twinning, perthites and graphic intergrowths	■	■	■	■	■	■	■	■
	II	subhedral	coarse	'comb' textures						■	■	
Plagioclase	I	subhedral to anhedral	medium to coarse	albite, pericline, albite-ala, albite-carlsbad twins. Myrmekitic intergrowths. Undulatory extinction, kinking, subgrains, 'mortar' textures with neoformed grains	■		■	■		■	■	■
	II	lamellar, vein, patch and bleb shapes	very fine to medium	perthitic 'lamellae'	■		■	■	■	■	■	■
	III	subhedral to anhedral	fine	'chess-board' albite			■	■		■	■	
	IV	subhedral	fine	'mantled textures'							■	
	V	subhedral to anhedra	very fine	'cleavelandite': saccharoidal							■	
Muscovite	I	euhedral to anhedral	fine to coarse	'book' textures, chevron domains, undulatory extinction, kinking	■	■	■	■	■	■		
	II	anhedral to fibrous-radial	very fine to medium	sericite: plag, Ksp and andalusite alteration product inter- and intragranular	■	■	■	■		■	■	■
	III	fibrous–needle texture	very fine to fine	crystals wrap around garnet, tourmaline, ...				■				
	IV	subhedral to anhedral	fine	'gilbertite': late interstitial mica							■	
	V	subhedral flakes	medium	foliaceous texture								■
Li-mica	I	prismatic fibrous-radial	fine to coarse	tri-dimensional frame, where the rest of the minerals are disposed							■	
	II	prismatic, fibrous-radial and dendritic	fine to coarse	inter- intragranular, in microfractures							■	
	III	granular	very fine	saccharoidal							■	
Andalusite		prismatic subhedral	fine to coarse	corundum inclusions, microfractures, reaction borders, sericite alteration		■		■				
Biotite		prismatic-tabular	fine to medium	frequently altered to chlorite	■		■	■		■		

TABLE 2 (*contd.*)

	Petrographic type	Shape and habit	Grain size	Textures and microstructures	Distribution *Pegmatite types							
					1	2	3	4	5	6	7	8
Tourmaline	I	prismatic-columnar euhedral to subhedral	fine to coarse	concentric chromatic zonation 'comb' textures	■	■	■	■		■		
Tourmaline	II	subhedral to anhedral	fine to medium	interstitial and in microfractures			■	■				
Tourmaline	III	prismatic, euhedral to subhedral	very fine to fine	poikiloblastic				■		■	■	■
Garnet		anhedral	fine	porphyroclasts		■		■				
Spodumene		euhedral to subhedral	fine to medium	frequently pseudomorphed by micas							■	
Apatite	I	subhedral to anhedral	fine to medium	sometimes broken		■		■		■	■	■
Apatite	II	subhedral	fine to medium	colourless to blueish in pleochroism						■		
Amblygonite Montebrasite		subhedral to anhedral	fine to coarse	polysynthetic twin, sometimes double						■	■	
Wyllieite-Rosemaryite		subhedral	fine	yellow to green in pleochroism						■		
Graftonite		subhedral	very fine	granular with sarcopside lamellae						■		
Sarcopside		subhedral	very fine	lamellae inside graft., ferrisickl., heter.						■		
Ferrisicklerite-Heterosite		subhedral	fine to medium	frequently lixiviated						■		
Sicklerite-Purpurite		euhedral to subhedral	very fine	granular							■	
Alluaudite		subhedral	fine	granular						■		
Triplite		subhedral	fine	granular						■		
Vayrynenite		anhedral	very fine	granular						■		
Columbite-Tantalite		euhedral to subhedral	very fine to coarse	granular, frequently together with cassiterite				■			■	■
Cassiterite		euhedral to subhedral	fine to coarse	'knee' twin, concnetric chromatic zonation						■	■	■
Rutile		prismatic-columnar	fine	together with cassiterite						■		
Corundum		bleb forms	very fine	as inclusions within andalusite		■						
Molybdenite		anhedral	fine to medium	frequently associated with cassiterite								■
Stannite		subhedral to anhedral	fine to medium	frequently associated with cassiterite							■	■
Pyrite		euhedral cubes	medium	granular					■	■		
Sphalerite		subhedral to anhedral	fine to medium	frequently associated with cassiterite							■	■
Calcite		anhedral	fine	granular						■		

schorl and minor andalusite, chlorite, garnet, biotite, apatite and columbite-tantalite (Fig. 2*d*). The host-rock frequently displays a strong tourmalinization near the contact. These dykes show an appreciable deformation, with flow textures, boudinage, and 'pinch and swell' structures. These pegmatites are located close to the Lumbrales granite.

Pegmatites mainly composed of K-feldspar (orthoclase and microcline) (T5)

Other phases that may be present are quartz, muscovite and pyrite. They are discordant to the host-rock, appearing near the contact with the Lumbrales granite.

Simple discordant pegmatites (T6)

In some cases these show a layered internal structure (Fig. 3*a*). They consist of quartz, K-feldspar (orthoclase and microcline), albite and muscovite. In the pegmatites nearest to the Lumbrales granite, a complex association of Fe-Mn phosphate minerals appears, such as wyllieite, graftonite, ferrisicklerite, sarcopside, alluaudite, triplite and heterosite, whereas in the distal pegmatites montebrasite may appear. K-feldspar can occur as coarse wedge-shaped crystals that grow perpendicular to the contacts with the host-rock and with their vertex pointing to the walls, which implies an oriented crystallization advancing from the margins of pegmatites inwards and a thermal gradient decreasing in the same direction. Situated in an area between 1 and 4 km to the north of the Lumbrales granite, this group is the most abundant.

Discordant Li-bearing pegmatites (T7)

Their shape is clearly dyke-like, striking N170° to N10°E and dipping close to vertical. Their maximum width is ~15 m, but thicknesses of <3 m are the most common. These bodies usually display a layered internal structure (Fig. 3*b*), with quartz and Li-mica bands alternating with other bands consisting of albite and K-feldspar, which suggests a non-linear model of crystallization. In these pegmatites, K-feldspar can occur as coarse wedge-shaped crystals that grow perpendicular to the contacts with the host-rock, inside the bands, in a manner similar to the T6 pegmatites. A number of bodies with zoned internal structure also belong to this group (Fig. 3*c*). They have a fine-grained border zone consisting of quartz, albite and minor montebrasite, a wall zone with albite and K-feldspar, and a core consisting of quartz and Li-mica. These dykes crop out along a narrow band, 4–6 km north of the Lumbrales granite.

Quartz pegmatites with abundant cassiterite (T8)

Fine-grained muscovite, microcline and albite are also present. Their shape is clearly dyke-like and, together with some of the T7 pegmatites, they form a stockwork hosted in the tourmalinized country-rock in the Feli open pit (Fig. 1). These dykes in some cases show internal zonation (Fig. 3*d*), generally with a border zone composed mainly of muscovite oriented parallel to the contacts; an intermediate zone consisting of microcline and albite, where fine to coarse grains of cassiterite may occur; and a core composed of quartz. Their thickness is usually <50 cm, striking similarly to the T7 pegmatites, and dipping at 45–65° to the east. These dykes are folded with a significant reduction in height. They appear in the north zone of the studied area.

Data collection and analyses

The blocky K-feldspars, micas, tourmalines, phosphates, Nb-Ta-Sn oxides and garnet analysed in this study were selected from the most representative pegmatites of the area. Micas, K-feldspar and tourmaline were separated by means of magnetic separation and hand-picking under a binocular microscope, with an estimated purity of ~99.5-99.7% in all the cases.

Trace-element analyses of micas and K-feldspar were performed by the X-ray Assay Labs of Don Mills, Ontario. Micas and blocky K-feldspar which were separated were analysed for Li by inductively coupled plasma (ICP) with 1 ppm as the detection limit; for Rb and Cs by instrumental neutron activation (INAA), both with 2 ppm as the detection limit; for Ba by ICP (1 ppm as the detection limit); and finally, K was analysed by XRF. Tourmalines, phosphates, Nb-Ta-Sn oxides and garnet were analysed for major elements at Paul Sabatier University (Toulouse, France), using a Camebax SX 50 electron microprobe. The operating conditions were: voltage of 15 kV and beam current of 20 nA. As internal standards $LiNbO_3$ for Nb, $LiTaO_3$ for Ta, titanite for Ti, SnO_2 for Sn, W metal for W, hematite for Fe, graftonite for Mn, albite for Na,

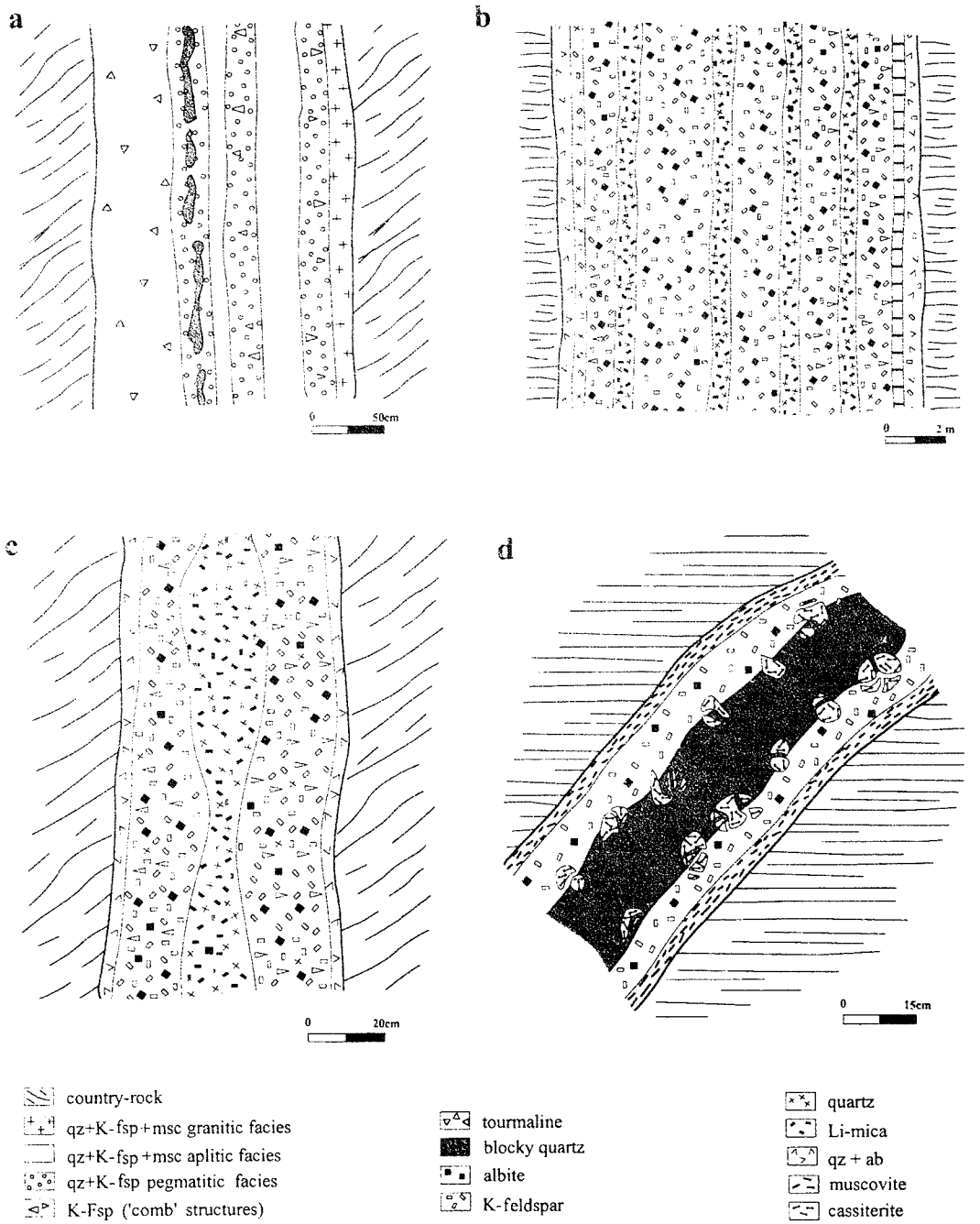

FIG. 3. Schematic section of some of the 'evolved' pegmatites; (*a*) simple discordant T6 pegmatite; (*b*) Li-bearing T7 pegmatite with layered internal structure; (*c*) Li-bearing T7 pegmatite with simple internal structure; and (*d*) Sn-bearing T8 dyke.

orthoclase for K, corundum for Al, wollastonite for Ca, MgO for Mg, and sphalerite for Zn were used. Whole-rock powders, as well as metasediments of the schist-metagreywacke complex, were analysed by XRF for Rb, Cs and Ba, and by AA for Li.

The structural states of K-feldspars were obtained by means of X-ray powder diffraction using Cu-$K\alpha$ radiation (λ = 1.5418 Å, 40 kV, 20 mA) and a graphite monochromator. Silicon and K-bromate were used as internal standards. Runs were made by scanning through 10–70° at 0.5°2θ min^{-1} for each sample. Preliminary indexing of each diffraction profile was based on the Borg and Smith (1969) data. Unit cell refinements were performed according to the procedure of Appleman and Evans (1973). Triclinicity was estimated according to the splitting between peaks 131 and $1\bar{3}1$ in X-ray powder patterns, so that triclinicity was calculated according to the Goldschmidt and Laves (1954) equation. Triclinic feldspars underwent an homogenization process at 1050°C for 48 h; and the composition of all the K-feldspars was calculated according to the most recent Hovis (1986) methods. Finally, the Al-Si distribution in the T sites was determined using the Kroll and Ribbe (1987) equations.

Mineralogy

In addition to the three major minerals of pegmatites: quartz, feldspar and mica, other minerals are present in variable amounts, e.g. tourmaline, cassiterite, columbite-tantalite, Fe-Mn-Li phosphates. The petrographic characteristics of all the recognized minerals are summarized in Table 2.

Feldspars

The textures and relative modal proportion of the feldspars vary depending on the pegmatite type, e.g. (1) the K-feldspar/plagioclase ratio decreases away from the Lumbrales granite, so that in the T7 and T8 pegmatites albite is more common than K-feldspar; (2) perthitic intergrowths appear in all pegmatites but they are more abundant in the less evolved pegmatites relative to the Li and Sn-bearing ones; (3) in the T6 and T7 pegmatites, K-feldspar shows a typical comb-structured growth orientation, including graphic intergrowths of quartz; (4) myrmekitic plagioclase-quartz intergrowths are restricted to this kind of pegmatite; and (5) in the T7 pegmatites K-feldspar, mantled by a cluster of plagioclase crystals, is observed.

The plagioclase composition ranges from An_0 to An_3. The Or content in K-feldspars varies from 87–100% according to the Hovis (1986) method. Microprobe analyses of the potassic matrix show that it contains very low concentrations of Na_2O (<0.1%) and CaO (<0.4%) (Table 3). The Al,Si ordering of K-feldspars corresponds to low microcline, intermediate microcline and orthoclase, $t_1 0 - t_1 m$ ranging from 0.0–0.94 (Table 3). A relation between the pegmatite type and the order degree of the K-feldspars has not been reported. Different order states of K-feldspars may coexist within the same pegmatite body (Table 3, Fig. 4). Orthoclase and/or intermediate microcline coexisting with low microcline and albite, suggests that the activity of hydrothermal fluids and tectonic stress gave rise to an uneven effect on the ordering in alkali feldspars.

Although variations in the major element contents for K-feldspar have not been detected, there are significant differences in the trace element contents depending on the pegmate type (Table 3 and Figs 4, 5). The feldspars associated with the less evolved T4 pegmatites are the poorest in Li, Rb and Cs, and show higher K/Rb ratios than those from the Li-rich T7 pegmatites, whereas these exhibit the feldspars richest in Li, among the richest in Rb and Cs, one of the poorest in Ba and with the lowest K/Rb ratios (Table 3) (Roda *et al.*, 1993). With regard to the T8 Sn-bearing pegmatites, their K/Rb ratio shows intermediate values, whereas their Ba and Sr contents are the highest (Figs 4, 5).

Micas

The main petrographic features of the micas are shown in Table 2 (for more detail, see Roda *et al.*, 1995*a*). The chemical data reveal compositional variations in the micas. These variations depend on the pegmatite type (Table 4). The trace elements contents such as those of Sn, Li, F, Cs, Rb, etc., seem to increase away from the Lumbrales granite, whereas there is an overall trend of decreasing Ba contents and K/Rb ratio in that direction (Fig. 5). Nevertheless, it is remarkable that in the case of micas associated with the T8 Sn-bearing pegmatites, their K/Rb ratio is intermediate, and one of the highest Ba contents is found in such a mica, as happens with the K-feldspar associated with these dykes.

TABLE 3. Chemical composition, *b* and *c* unit cell parameters, structural parameters and Or contents of the studied feldspars (%Or according to the Hovis method (1986))

	*T1-1	T1-2	T1-3	T1-4	T3-1	T3-2	T3-3	T4-1	T4-2	T5-1	T6-1	T6-2	T6-3	T6-4	T6-5	T6-6	T6-7	nnT6-8	T7-1	T7-2	T7-3	T7-4	T7-5	T8-1
K_2O	16.14	16.02	15.66	15.78	15.66	14.70	14.82	15.54	16.14	15.78	15.54	16.14	15.90	16.02	16.14	15.78	15.78	17.83	17.11	16.74	14.94	15.66	15.66	14.94
CaO	0.06	0.13	0.08	0.24	0.08	0.13	0.10	0.07	0.14	0.38	0.10	0.06	0.11	0.10	0.20	0.08	0.13	0.04	0.10	0.06	0.11	0.10	0.13	0.70
FeO	0.01	0.01	0.01	0.03	0.01	0.03	0.01	0.01	0.01	0.04	0.05	0.01	0.01	0.01	0.05	0.06	0.01	0.01	0.01	0.01	0.01	0.01	0.01	0.01
Na_2O	0.00	0.01	0.01	0.00	0.01	0.00	0.01	0.00	0.01	0.00	0.00	0.00	0.00	0.00	0.01	0.00	0.00	0.00	0.00	0.00	0.00	0.00	0.00	0.00
SiO_2	65.58	67.01	66.48	65.42	66.95	67.55	66.82	66.64	66.86	66.27	67.01	65.59	65.75	64.96	66.69	66.52	65.39	65.37	65.91	65.78	67.48	66.89	66.99	67.78
Al_2O_3	17.19	16.21	16.93	17.61	16.53	17.18	17.52	17.29	16.25	16.85	17.06	17.19	17.02	17.93	16.55	17.31	17.33	16.55	16.72	16.93	16.91	16.82	16.61	16.51
MgO	0.03	0.05	0.05	0.03	0.05	0.03	0.05	0.03	0.05	0.03	0.03	0.02	0.03	0.03	0.05	0.02	0.03	0.02	0.03	0.02	0.02	0.02	0.03	0.03
Total	99.02	99.43	99.23	99.11	99.30	99.61	99.32	99.59	99.46	99.36	99.80	99.02	98.84	99.06	99.68	99.77	98.67	99.82	99.89	99.54	99.47	99.50	99.43	99.98
Number of cations on the basis of 32 atoms of oxygen																								
Si	12.202	12.385	12.292	12.145	12.362	12.348	12.270	12.263	12.368	12.265	12.302	12.204	12.237	12.085	12.316	12.242	12.188	12.200	12.229	12.219	12.371	12.327	12.353	12.387
Al	3.772	3.533	3.690	3.854	3.599	3.701	3.792	3.750	3.544	3.677	3.693	3.772	3.736	3.932	3.604	3.755	3.807	3.642	3.657	3.707	3.655	3.653	3.611	3.558
Fe^{2+}	0.002	0.002	0.002	0.004	0.002	0.004	0.002	0.002	0.002	0.006	0.008	0.002	0.002	0.002	0.008	0.010	0.002	0.002	0.002	0.002	0.002	0.002	0.002	0.002
Mg	0.009	0.014	0.014	0.009	0.014	0.009	0.014	0.009	0.014	0.009	0.009	0.005	0.009	0.009	0.014	0.005	0.009	0.005	0.009	0.005	0.005	0.005	0.009	0.009
Ca	0.011	0.025	0.017	0.047	0.017	0.025	0.019	0.014	0.028	0.075	0.019	0.011	0.022	0.020	0.039	0.017	0.025	0.008	0.019	0.011	0.022	0.019	0.025	0.137
Na	0.001	0.002	0.002	0.001	0.002	0.001	0.002	0.001	0.002	0.001	0.001	0.001	0.001	0.001	0.002	0.001	0.001	0.001	0.001	0.001	0.001	0.001	0.001	0.001
K	3.832	3.778	3.694	3.737	3.689	3.427	3.471	3.648	3.810	3.726	3.640	3.832	3.776	3.802	3.803	3.705	3.752	4.245	4.049	3.968	3.493	3.682	3.684	3.483
Z	15.973	15.918	15.982	15.999	15.961	16.049	16.062	16.013	15.911	15.942	15.995	15.976	15.973	16.017	15.919	15.997	15.995	15.842	15.887	15.926	16.026	15.980	15.963	15.945
X	3.855	3.821	3.728	3.799	3.723	3.466	3.508	3.674	3.855	3.817	3.677	3.850	3.811	3.834	3.866	3.737	3.790	4.261	4.081	3.986	3.523	3.708	3.721	3.632
%Or	95.4	94.7	92.5	93.3	92.5	86.8	87.6	91.8	95.4	93.3	91.8	95.4	94.0	94.7	95.4	93.3	93.3	99.79	99.5	99.0	88.3	92.5	92.5	88.3
Li	17	26	14	26	8	2	6	6	1	1	9	12	28	11	48	32	21	2	29	31	202	218	171	9
Be	5	2	6	8	6	1	5	3	1	5	13	8	12	7	15	11	12	1	4	6	4	3	4	1
Cu	1	1	1	1	0	0	0	0	0	1	1	0	1	1	1	1	1	1	0	1	1	1	0	1
Zn	5	4	3	3	2	4	1	1	1	1	7	10	2	8	6	8	7	1	4	6	5	6	5	1
Rb	1300	800	800	900	2000	600	1000	500	600	1000	1900	2600	3000	3400	1400	1900	4400	3000	3400	2900	4000	3900	4700	1000
Sr	13	13	26	25	8	45	22	15	33	126	12	24	13	12	42	19	24	9	32	28	34	32	31	536
Y	0	0	0	0	0	0	0	0	0	1	0	0	0	0	1	0	0	0	0	0	0	0	0	0
Zr	2	4	2	1	3	2	2	2	2	1	1	0	1	1	2	0	1	0	2	0	1	1	1	0
Nb	1	2	0	1	0	0	0	0	0	0	0	0	0	0	0	1	0	2	1	0	0	1	0	0
Sn	15	10	11	10	13	10	12	10	13	10	10	10	22	13	10	10	21	10	10	10	10	10	10	10
Cs	70	36	53	74	42	10	86	7	28	30	40	34	64	124	29	38	280	154	141	137	106	713	401	174
Ba	32	17	46	17	13	104	31	27	62	253	72	33	16	15	53	57	30	45	44	19	5	13	9	971
Pb	8	11	33	2	8	43	23	63	34	11	2	34	2	6	2	2	2	2	2	24	14	38	47	129
Bi	9	8	14	5	8	8	6	7	9	5	8	7	6	9	8	3	4	3	10	8	6	8	9	9
K/Rb	103	167	162	145	65	204	123	258	224	131	68	52	44	39	96	69	30	49	42	48	31	33	28	124
Rb/Sr	100	62	31	36	250	13	45	33	18	8	158	108	231	283	33	100	183	333	106	104	118	122	152	2
b	12.990	12.963	12.973	12.986	12.984	12.964	12.986	12.963	12.970	12.956	12.945	12.979	12.996	12.977	12.965	12.950	12.985	12.965	12.968	12.985	12.978	12.985	12.973	12.945
	(3)	(3)	(5)	(3)	(4)	(6)	(3)	(5)	(1)	(7)	(3)	(3)	(3)	(2)	(7)	(7)	(3)	(6)	(4)	(5)	(7)	(5)	(3)	(5)
c	7.200	7.215	7.197	7.194	7.200	7.209	7.217	7.209	7.210	7.206	7.213	7.196	7.192	7.195	7.220	7.215	7.191	7.233	7.224	7.204	7.193	7.218	7.20	7.216
	(1)	(1)	(2)	(1)	(2)	(2)	(1)	(2)	(6)	(3)	(1)	(1)	(1)	(1)	(3)	(3)	(1)	(3)	(2)	(2)	(3)	(2)	(2)	(2)
t1o+t1m	0.77	0.93	0.81	0.77	0.81	0.91	0.80	0.90	0.90	0.93	1.01	0.79	0.72	0.80	0.96	1.01	0.77	1.04	0.96	0.81	0.75	0.86	0.90	1.02
t1o-t1m	–	0.90	–	–	–	0.87	0.67	–	0.87	0.04	0.83	–	–	–	0.93	0.80	–	0.00	0.94	–	–	0.81	−0.47	0.89
A	0	0.77	0	0	0	0.81	0.62	0	0.82	0.12	0.82	0	0	0	0.87	0.80	0	0.74	0.93	0	0	0.66	0.47	0.86

(*Pegmatite types numbered as in Fig. 1)

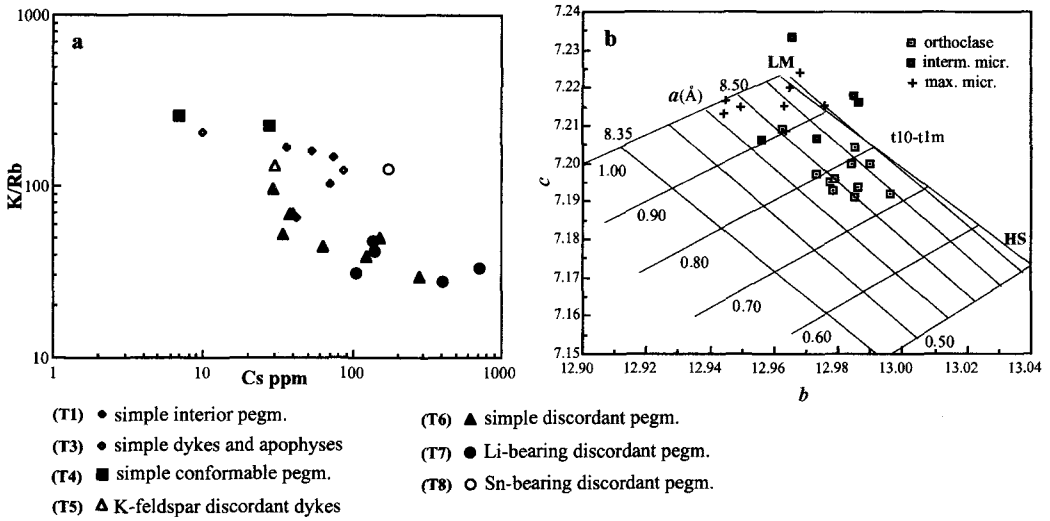

FIG. 4. (*a*) Plot of the K/Rb ratio *vs* Cs contents in some of the studied K-feldspars (values in ppm); and (*b*) *b*–*c* cell dimensions plot for the studied K-feldspars. LM (low microcline), HS (high sanidine) points and cross contoured for tlo-tlm are from Kroll and Ribbe (1983). *a* values are from Wright and Stewart (1968).

TABLE 4. Mica compositional data, and whole-rock (WR) compositions calculated according to the procedure of Shearer *et al.*, 1992

Pegm. type	(T1)	(T1)	(T1)	(T1)	(T1)	(T2)	(T3)	(T3)	(T3)	(T4)	(T4)	(T4)	(T4)	(T4)	(T4)
Ba ppm	26	16	118	131	10	321	258	262	259	318	632	717	287	237	447
Rb ppm	1200	2000	2240	800	1400	1335	3000	2990	1372	1451	1014	847	1441	1393	560
Li ppm	383	345	425	294	434	158	158	367	152	32	93	36	65	51	251
Cs ppm	151	199	141	63	153	–	205	265	210	–	–	–	–	19	–
K/Rb	54	36	32	99	61	61	26	28	64	56	81	90	56	57	99
Rb/Sr	200	286	–	89	233	–	–	–	–	–	400	11	1441	1393	–
Ba (WR)	7	4	32	35	3	87	70	71	70	86	171	194	78	64	121
Rb (WR)	857	1428	1600	571	1000	953	2143	2136	981	1036	724	605	1029	995	400
Li (WR)	479	431	532	367	542	197	197	459	190	40	116	45	81	64	314

Pegm. type	(T6)	(T6)	(T6)	(T6)	(T6)	(T6)	(T6)	(T7)	(T7)	(T7)	(T7)	(T7)	(T7)	(T8)	(T8)
Ba ppm	165	395	248	632	284	321	274	361	392	476	11	74	16	175	657
Rb ppm	4012	4492	4675	3995	3866	5519	3538	8108	8397	9181	6900	7479	7200	1700	1887
Li ppm	339	341	725	344	386	350	409	13565	16260	22253	14000	14417	13400	1160	492
Cs ppm	–	40	40	66	262	265	484	1559	1565	1696	1540	1538	1500	335	137
K/Rb	20	18	18	20	21	15	23	10	10	9	11	10	8	46	46
Rb/Sr	4012	1497	1558	400	1290	1104	884	737	840	1020	238	–	167	57	29
Ba (WR)	45	107	67	170	77	87	74	98	106	128	3	20	4	47	178
Rb (WR)	2866	3209	3339	2854	2761	3942	2527	5791	5998	6557	4929	5342	5143	1214	1348
Li (WR)	429	429	906	430	482	430	511	3768	4517	6181	3889	4005	3722	1450	616

(* numbers of the pegmatite types as in Table 1)

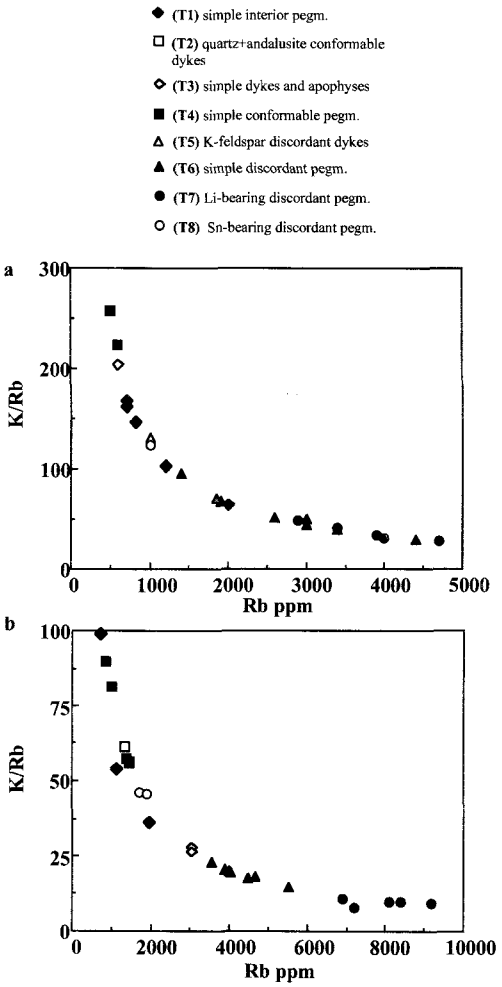

FIG. 5. K/Rb *vs* Rb of the K-feldspar (*a*), and micas (*b*), in the different pegmatite types of the Fregeneda area.

TABLE 5. Chemical composition of garnets from the simple T4 concordant pegmatites

n*	(T4)-1 6	(T4)-2 6
SiO_2	35.96	35.81
Al_2O_3	20.55	20.65
Fe_2O_3	1.32	1.85
FeO	28.73	29.06
MnO	12.09	12.02
MgO	0.80	0.65
CaO	0.43	0.24
Na_2O	0.00	0.01
Total	99.89	100.31
Number of cations on the basis of 12 atoms of oxygen		
Si	2.962	2.944
Al	0.038	0.056
Sum	3.000	3.000
Al	1.958	1.946
Fe^{3+}	0.082	0.114
Sum	2.039	2.060
Mg	0.098	0.080
Fe^{2+}	1.980	1.998
Mn	0.844	0.837
Ca	0.038	0.021
Na	0.000	0.002
Sum	2.959	2.938

*number of point analyses

Tourmaline

Textural and paragenetic differences among the tourmaline samples from the various types of pegmatite have been observed (Table 2). All the tourmaline samples analysed belong to the schorl–dravite series, mainly the Fe^{2+}-rich end-member. Nevertheless, the data show compositional variations that correlate with the pegmatite type (Roda *et al.*, 1995*b*). It is also remarkable that in no case has a difference between the composition of tourmalines from the core and from the wall of the same body of pegmatite been found. In general, tourmaline from the T6 pegmatites has the highest Fe/Mg value, whereas tourmaline from the quartz and andalusite dykes (T2) show the lowest Fe/Mg value (Roda *et al.*, 1995*b*).

Garnet

Garnet was found only in the simple concordant T4 pegmatites with mylonitic texture. It appears as fine-grained, rounded, frequently fractured crystals. Chemically it corresponds to an intermediate member of the almandine-spessartine series, with a higher Fe than Mn content (Table 5). Representation of the data on the MgO-FeO-MnO ternary diagram (Černý and Hawthorne, 1982) falls at the intersection of the compositional field of muscovite formations and that of muscovite + rare element pegmatites (Fig. 6).

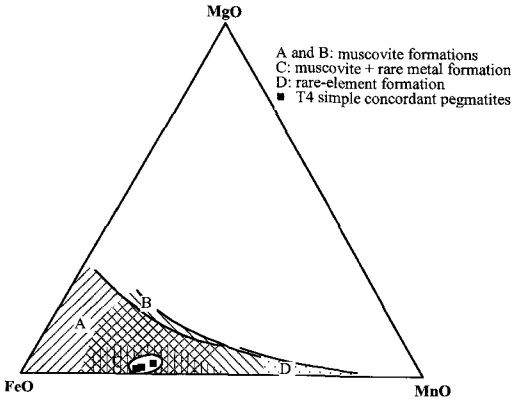

FIG. 6. MgO-FeO-MnO values of the garnets from the simple concordant T4 pegmatites. (Compositional fields of garnets from different pegmatite types from Černý and Hawthorne (1982), from data of other authors).

Andalusite

Andalusite appears in the T2 bodies, where it is a main component, and in some T4 pegmatites, mainly in those showing mylonitic textures, where it appears as an accessory mineral. Two different petrographic types have been distinguished. The first one is an euhedral, fine- to coarse-grained andalusite, which usually shows inclusions of corundum. It may be fractured, and partly replaced by sericite along the fractures. In hand specimen it shows a prismatic habit with brown, pinkish or dark-green colours. The second petrographic type corresponds to an anhedral, fine-grained andalusite, which is strongly replaced by sericite. Both petrographic types are chemically similar, with an FeO content of <1 wt.%.

Phosphates

These occur mainly in the T6 pegmatites, which are located in an intermediate zone, between the barren pegmatites and the most evolved Li and Sn-bearing bodies (Table 2). The study of these phosphates has shown a complex association of Fe-Mn phosphate minerals (Roda *et al.*, 1996). The primary identified phases are wyllieite, graftonite, sarcopside, ferrisicklerite, triplite and Mn-rich apatite; and the secondary phosphates are heterosite, rosemaryite, alluaudite and vayrynenite. In the Li-bearing T7 pegmatites, Fe-Mn-phosphates are rare, but sicklerite and purpurite (the Mn-rich members of the sicklerite-ferrisicklerite and purpurite-heterosite series respectively) have been found. However, montebrasite is present in the T7 pegmatites as well as in some T6 dykes, mainly in those further from the Lumbrales granite. According to the pegmatite type, chemical differences have been noted in this phase; montebrasite associated with T7 pegmatites being richer in F and poorer in P than that associated with the T6 dykes.

Nb-Ta-Sn minerals

Columbite-tantalite has been found only in the T4, T7 and T8 pegmatites. In the T4 pegmatites it is very rare, appearing together with quartz, K-feldspar, plagioclase, muscovite, garnet and apatite. In this case it appears as very fine-grained subhedral crystals. In the T7 pegmatites columbite-tantalite usually occurs as fine-grained subhedral crystals, associated with cassiterite. Less commonly it appears as euhedral crystals (up to 1 cm in length) growing in a fine-grained matrix consisting of muscovite, quartz and plagioclase. Finally, in the T8 pegmatites, columbite-tantalite is always associated with cassiterite, appearing as sub- to anhedral fine-grained crystals.

Its chemical composition ranges from ferrocolumbite in the T4 and T8 pegmatites to manganocolumbite in the T7 pegmatites, with a greater enrichment in Mn than Ta (Table 6, Fig. 7). The most extreme Mn enrichment in manganocolumbite occurs in the T7 Li-bearing pegmatites, whereas the Sn-bearing T8 dykes are the poorest in Mn and the richest in Fe. An overall trend of increasing Ta/(Ta+Nb) in columbite-tantalite from T7 dykes has also been observed. However, in contrast to the increase of the Mn/(Mn+Fe) ratio, the increase in Ta/(Ta+Nb) is subordinate, and the dominant trend is of Mn enrichment. In all cases the TiO_2 contents are relatively low, columbite from the T4 dykes showing the highest values (3.06 wt.%) and that from Li-bearing T7 dykes being the lowest (0.34 wt.%). Finally, there is minor variation in Sn contents, which are very low (<0.72 wt.%) (Table 6).

The main Sn-bearing mineral found in these pegmatites is cassiterite (Table 2). It occurs in T6 pegmatites (but only in those closer to the Lumbrales granite), in Li-bearing T7 dykes, and mainly in Sn-bearing T8 pegmatites, which have been mined in the Feli open pit for some decades.

TABLE 6. Chemical composition of some columbite-tantalite from the simple concordant T4 pegmatites, the Li-bearing T7 pegmatites and the Sn-bearing T8 pegmatites (*dark sample, **light sample)

	T4	T7	T7	T7	T7	T7	T7*	T7	T7**	T7	T7	T8	T8	T8
Nb_2O_5	53.10	37.91	36.90	37.53	39.08	52.52	60.73	38.53	41.07	49.99	38.50	69.23	66.92	71.54
Ta_2O_5	23.09	44.41	45.26	42.93	42.78	27.69	20.11	43.73	39.09	30.50	43.03	7.70	8.39	7.01
FeO	13.95	1.10	0.81	1.06	1.44	0.84	1.05	0.68	0.95	0.99	1.33	17.93	16.85	18.61
MnO	3.46	15.33	15.54	15.52	15.87	17.07	18.55	15.90	15.40	16.90	15.18	2.11	2.60	1.46
SnO_2	0.07	0.72	0.50	0.76	0.39	0.39	0.21	0.48	0.50	0.38	0.68	0.46	0.32	0.60
TiO_2	3.47	0.47	0.34	0.63	0.46	0.39	0.41	0.36	0.40	0.38	0.35	1.80	1.47	2.14
CuO	0.00	0.00	0.00	0.00	0.00	0.00	0.00	0.00	0.00	0.00	0.00	0.00	0.00	0.00
Sc_2O_3	0.94	0.09	0.12	0.06	0.09	0.06	0.00	0.11	0.07	0.04	0.09	0.00	0.00	0.00
WO_3	1.39	0.00	0.00	0.00	0.00	0.00	0.00	0.00	0.00	0.00	0.22	0.00	0.00	0.00
Total	99.47	100.03	99.47	98.50	100.11	98.95	101.06	99.78	97.47	99.18	99.38	99.23	96.53	101.36
Number of cations on the basis of 6 atoms of oxygen														
Nb	1.471	1.164	1.146	1.166	1.191	1.510	1.653	1.183	1.267	1.453	1.185	1.817	1.814	1.829
Ta	0.385	0.820	0.845	0.803	0.784	0.479	0.329	0.807	0.726	0.533	0.797	0.122	0.137	0.108
Fe	0.715	0.062	0.046	0.061	0.081	0.044	0.053	0.039	0.054	0.053	0.076	0.871	0.845	0.880
Mn	0.180	0.882	0.904	0.904	0.906	0.920	0.946	0.914	0.890	0.921	0.876	0.104	0.132	0.070
Sn	0.002	0.019	0.014	0.021	0.011	0.010	0.005	0.013	0.014	0.010	0.018	0.011	0.008	0.014
Ti	0.160	0.024	0.018	0.033	0.024	0.019	0.019	0.018	0.020	0.018	0.018	0.079	0.066	0.091
Cu	0.000	0.000	0.000	0.000	0.000	0.000	0.000	0.000	0.000	0.000	0.000	0.000	0.000	0.000
Sc	0.050	0.006	0.007	0.004	0.005	0.003	0.000	0.006	0.004	0.002	0.005	0.000	0.000	0.000
W	0.022	0.000	0.000	0.000	0.000	0.000	0.000	0.000	0.000	0.000	0.004	0.000	0.000	0.000

In the T6 pegmatites cassiterite is scarce, and it is always associated with rutile. It appears as subhedral crystals, up to 1 cm long, which often show the familiar geniculate twin. It usually shows a chromatic zonation, with alternating dark (strong pleochroism ranging from dark-brown to reddish-brown) and pale bands (light-brown to yellow pleochroism).

Cassiterite in Li-bearing T7 pegmatites occurs as fine-grained zoned crystals. In some cases it appears as euhedral crystals growing in a fine-grained matrix consisting of muscovite, quartz and plagioclase. In other cases, it is found associated with quartz and other oxides and sulphides (columbite-tantalite, stannite, sphalerite) showing subhedral habit. In both cases, cassiterite shows a chromatic zonation, and the pleochroism of the crystals associated with other oxides and sulphides is stronger than that of the euhedral crystals.

The Sn-bearing T8 dykes are the richest in cassiterite. It appears as fine- to coarse-grained crystals (in some cases up to 7 cm across), associated with other oxides and sulphides (columbite-tantalite, stannite, sphalerite, chalcopyrite, molybdenite, galena). Crystals are

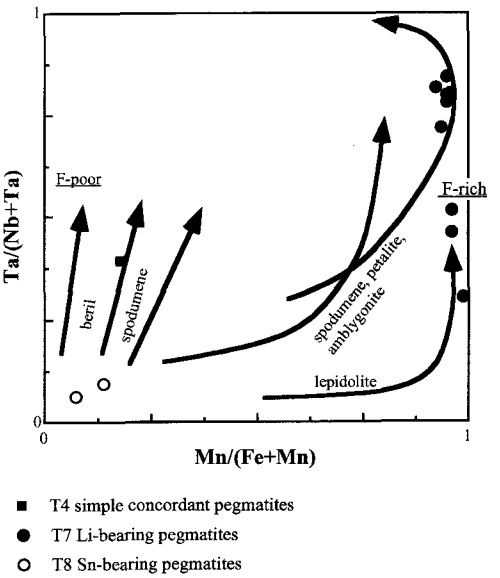

FIG. 7. Plot of Mn/(Fe+Mn) *vs* Ta/(Nb+Ta) for the columbite-tantalite analysed. (Fractionation lines for columbite-tantalites are from Černý (1992), modified from Černý (1989)).

commonly sub- to euhedral and frequently they are broken, with a 'puzzle' texture. As in the T6 pegmatites, cassiterite also shows geniculate twinning in T8 dykes. Chromatic zonation is observed in many crystals, with alternating dark and pale ribbons, the pleochroism in all cases being less intense than in the cassiterites from the T6 pegmatites.

As with the columbite-tantalite, there are also compositional differences between the cassiterites from the different types of pegmatites (Table 7). Those from T8 pegmatites are the poorest in Ta_2O_5 (<0.82 wt.%) and the richest in Nb_2O_5 (up to 2.04 wt.%). Cassiterites from T6 pegmatites have the highest concentrations of Ta_2O_5 (>2.23 wt.%) and the lowest SnO_2

TABLE 7. Chemical composition of cassiterites from the simple discordant T6 pegmatites, the Li-bearing T7 pegmatites and the Sn-bearing T8 dykes

	T6-1	T6-2	T6-3	T7-1	T7-1B	T7-2	T7- C1	T7-C2	T7-C3
Nb_2O_5	0.00	0.79	0.30	0.69	0.40	0.80	0.70	0.23	0.52
Ta_2O_5	4.70	3.38	2.23	0.89	2.14	0.24	1.23	0.21	1.55
FeO	0.70	0.63	0.44	0.27	0.48	0.16	0.33	0.00	0.32
MnO	0.20	0.02	0.00	0.00	0.03	0.01	0.00	0.00	0.00
SnO_2	94.40	93.76	94.97	98.16	97.05	98.87	98.18	98.73	97.49
TiO_2	0.00	0.26	0.25	0.10	0.06	0.00	0.02	0.02	0.04
CuO	–	–	–	–	–	0.02	–	0.11	–
Total	100.00	98.85	98.19	100.10	100.15	100.09	100.46	99.30	99.92
Number of cations on the basis of 2 atoms of oxygen									
Nb	0.000	0.009	0.004	0.008	0.005	0.009	0.008	0.003	0.006
Ta	0.032	0.023	0.016	0.006	0.015	0.002	0.008	0.001	0.011
Fe	0.015	0.013	0.009	0.006	0.010	0.003	0.007	0.000	0.007
Mn	0.004	0.000	0.000	0.000	0.001	0.000	0.000	0.000	0.000
Sn	0.950	0.948	0.967	0.978	0.970	0.985	0.976	0.993	0.975
Ti	0.000	0.005	0.005	0.002	0.001	0.000	0.000	0.000	0.001
Cu	0.000	0.000	0.000	0.000	0.000	0.000	0.000	0.002	0.000

	T7-B	T8-1	T8-2	T8-3	T8-4	T8-5	T8-Br	T8-Cr	T8-cl
Nb_2O_5	0.46	0.70	0.33	1.69	0.22	0.23	0.87	0.89	2.04
Ta_2O_5	1.35	0.35	0.82	0.29	0.38	0.55	0.34	0.31	0.62
FeO	0.36	0.22	0.25	0.45	0.15	0.10	0.42	0.37	0.70
MnO	0.02	0.00	0.00	0.00	0.00	0.05	0.00	0.00	0.00
SnO_2	97.36	96.28	97.12	95.03	98.47	99.03	97.94	97.15	95.28
TiO_2	0.12	0.32	0.26	0.20	0.40	0.20	0.37	0.28	0.28
CuO	–	–	–	–	–	–	–	–	–
Total	99.68	97.87	98.77	97.66	99.62	100.14	99.93	99.00	98.92
Number of cations on the basis of 2 atoms of oxygen									
Nb	0.005	0.008	0.004	0.019	0.002	0.003	0.010	0.010	0.023
Ta	0.009	0.002	0.006	0.002	0.003	0.004	0.002	0.002	0.004
Fe	0.008	0.005	0.005	0.010	0.003	0.002	0.009	0.008	0.015
Mn	0.000	0.000	0.000	0.000	0.000	0.001	0.000	0.000	0.000
Sn	0.976	0.978	0.981	0.965	0.985	0.987	0.974	0.975	0.953
Ti	0.002	0.006	0.005	0.004	0.007	0.004	0.007	0.005	0.005
Cu	0.000	0.000	0.000	0.000	0.000	0.000	0.000	0.000	0.000

B = border; C = core; r = reddish; cl = clear

(<94.97 wt.%), whereas those from the Li-bearing T7 pegmatites have the highest concentrations of SnO_2 (>97.05 wt.%) and show the lowest of Nb_2O_5+Ta_2O_5 (<2.54 wt.%). The TiO_2 values are very low, in general <0.37 wt.%, but an overall trend of increasing TiO_2 in the cassiterite from the border to the core in the T7 and T8 pegmatites has been observed. A relation between composition and colour has also been observed, with reddish bands having higher Nb, Ta and Fe contents, whereas pale bands have higher Ti contents.

Li, Rb and Ba contents in granitic rocks

In general, the high Li contents in the granites of this area, (leucogranites as well as calc-alkaline granites) are noteworthy. The Lumbrales granite, the closest to the studied pegmatites, is a two-mica leucogranite with Li contents, greater than the average values established for these types of rocks, of ~40 ppm (Beus, 1960; Heier and Adams, 1964) (Table 8). Likewise, the high Rb content is remarkable, exceeding by more than 100 ppm the general values of Rb in granites, which are typically <200 ppm (Hedge, 1966). Equally remarkable is the low Ba content found in this body. The K/Rb ratio is also low, with values of <160 ppm (Bea, 1976; Bea and Ugidos, 1976), characteristic of pegmatoids and very differentiated granites (Ahrens *et al.*, 1952). In relation to the studied pegmatites, the Li, Rb and Ba contents of the Lumbrales granite are very similar to those of the T4 pegmatites, which appear to be the less evolved. All the rest of the pegmatite types are, in general, richer in Li and Rb and poorer in Ba than the Lumbrales granite.

TABLE 8. Trace element data and mineral modes (vol. %) for the Lumbrales granite (L-G) and rocks from the schist-metagreywacke complex (CEG)

	L-G	CRG-1	CEG-2
Li ppm	118(32–233)[(1)]	161	100
Rb ppm	343(263–449)[(1)]	180	292
Ba ppm	218(88–618)[(1)]	835	713
Sr ppm	56(34–75)[(1)]	–	–
K/Rb	128(88–172)[(1)]	–	–
Quartz	46	25	40
K-felds	22	13	12
Albite	18	–	20
Biotite	4	55	–
Muscovite	10	8	–
Sillimanite	–	–	14
Garnet	–	–	1

[(1)] data from Bea and Ugidos (1976). Average from 150 analyses. In parentheses: ranges of values.

Trace element modelling

The nature, distribution and textural relationships of mineral assemblages and their mineral chemistry have been used to evaluate the petrogenetic link between pegmatites and their associated granites (Černý and Meintzer, 1988; Shearer *et al.*, 1985; Jolliff *et al.*, 1986, 1987, 1992; Norton and Redden, 1990; Roda *et al.*, 1995*a,b*).

The contents of Ba, Rb and Li in mica and K-feldspar, and some bulk chemical analysis of pegmatite rocks, have been used to establish the petrogenetic links between the different pegmatite types and the granites of the area. In order to estimate the initial trace element concentration of the parent melt, trace element concentrations in muscovite and K-feldspar have been used according to the Jolliff *et al.* (1992) method. This method applies the mass-balance equation: $C_{total} = f_{solid}*C_{solid} + f_{liquid}*C_{liquid}$. The values calculated by this method agree with those obtained by whole-rock XRF analysis (Table 9).

The distribution of trace elements between solid and melt in high-silica systems is imprecise, and consequently, there is controversy in the selection of the crystal/liquid partition coefficients. The data show a wide variation, which may sometimes change the obtained crystallization paths. In this case, some of the partition coefficients employed in trace element modelling (fractional crystallization) (Table 10) have been used previously by Jolliff *et al.* (1992) in their study of the petrogenetic relationships between pegmatites and granites in the Black Hills (Dakota, USA). The other partition coefficients, used in the modelling of the partial melting of the metasedimentary rocks, have been compiled by Walker *et al.* (1989).

Fractional crystallization may explain the wide variation of pegmatite compositions observed in many pegmatite fields. The compositions of melts derived by different degrees of fractional crystallization of parent melts with the composition of the Lumbrales granite are illustrated in Fig. 8. Thus, using Ba as a compatible trace element, and

TABLE 9. Comparison of the Ba, Rb and Li contents (ppm) of the pegmatites of the Fregeneda area: (1) XRF data; (2) calculated values obtained by applying the Jolliff *et al.* (1992) method, using the mica contents coupled with relevant partition coefficients

Pegm. type	Ba		Rb		Li
	(1)	(2)	(1)	(2)	(2)
T1	14–28	3–35	909	571–1600	367–542
T2	83–96	87	850–1010	953	197
T3	78	70–71	2045	981–2143	190–459
T4	55–90	64–194	598–1100	400–1036	40–314
T6	50–130	45–170	2601–3576	2527–3942	429–906
T7	19–61	3–128	3532–8509	4929–6557	3722–6181
T8	45–120	47–178	1038–1264	1214–1348	616–1450

Rb and Li as incompatible trace elements, Ba concentrations decrease with the fractional crystallization whereas Li and Rb increase. Therefore, the more evolved pegmatites correspond to the later stages of fractional crystallization, and are enriched in incompatible elements.

Some authors have proposed a metamorphic-anatectic model for the genesis of rare-element pegmatites (Stewart, 1978; Norton, 1981; Sokolov, 1981; Shmakin, 1983; Shearer *et al.*, 1987*a*). A partial melting model involves varying degrees of partial melting to generate the broad compositional range of many of the granite-pegmatite fields. High degrees of partial melting will produce granitic rocks, whereas smaller degrees of partial melting will produce the more evolved pegmatites. The path followed by the partial melting of metasediments with similar Li, Rb and Ba contents (Table 8) to those shown by the metasediments of the schist-metagreywacke complex from the Fregeneda area is illustrated in Fig. 8. One example shows the trajectory of a partial melt with a biotite-bearing residue. As a result of the affinity shown by this mineral for trace elements such as Li and Rb, the melt produced is poorer in those elements than the protolith. Thus, this mechanism cannot generate evolved pegmatites. However, for a biotite-absent residue, the partial melt is richer in rare alkalis than the protolith, with low degrees of melting.

For modelling purposes, the Li, Rb and Ba concentrations of a hypothetical source rock are assumed to lie within the compositional range of metasedimentary rocks of the schist-metagreywacke complex, because of the general similarity of trace element compositions for pelitic rocks (Gromet *et al.*, 1984; Bathia and Crooks, 1986). Moreover, the compositional variation within the metasedimentary suite is minor compared to the variation between the suite and the estimated compositions of the pegmatites (Walker *et al.*, 1989). High degrees of partial melting (>50%) would result in the production of large volumes of granitic melt with low concentrations of rare-alkali elements, whereas smaller degrees of partial melting (<25%) would generate granitic

TABLE 10. Partition coefficients used: (a) in the modelling of the fractional and equilibrium crystallization; and (b) in the modelling of the partial melting of a metasedimentary rock

	K-feldspar	Albite	Biotite	Quartz	Garnet	Sillim.
Ba	$6_{ab}^{(1,2)}$	$0.3_a^{(1)}\ 0.27_b^{(2)}$	$6.4_{ab}^{(1)}$	$0.025_a^{(1)}\ 0_b^{(2)}$	$0.02_b^{(2)}$	$0_b^{(2)}$
Rb	$0.7_a^{(1)}\ 0.31_b^{(2)}$	$0.1_a^{(1)}\ 0.04_b^{(2)}$	$4_{ab}^{(1)}$	$0.01_a^{(1)}\ 0_b^{(2)}$	$0.01_b^{(2)}$	$0_b^{(2)}$
Li	$0.05_{ab}^{(1,2)}$	$0.05_a^{(1)}0.1_b^{(2)}$	$3.6_{ab}^{(1)}$	$0.05_a^{(1)}0_b^{(2)}$	$0_b^{(2)}$	$0_b^{(2)}$

(1) Data complied by Jolliff *et al.* (1992)
(2) Data compiled by Walker *et al.* (1989).

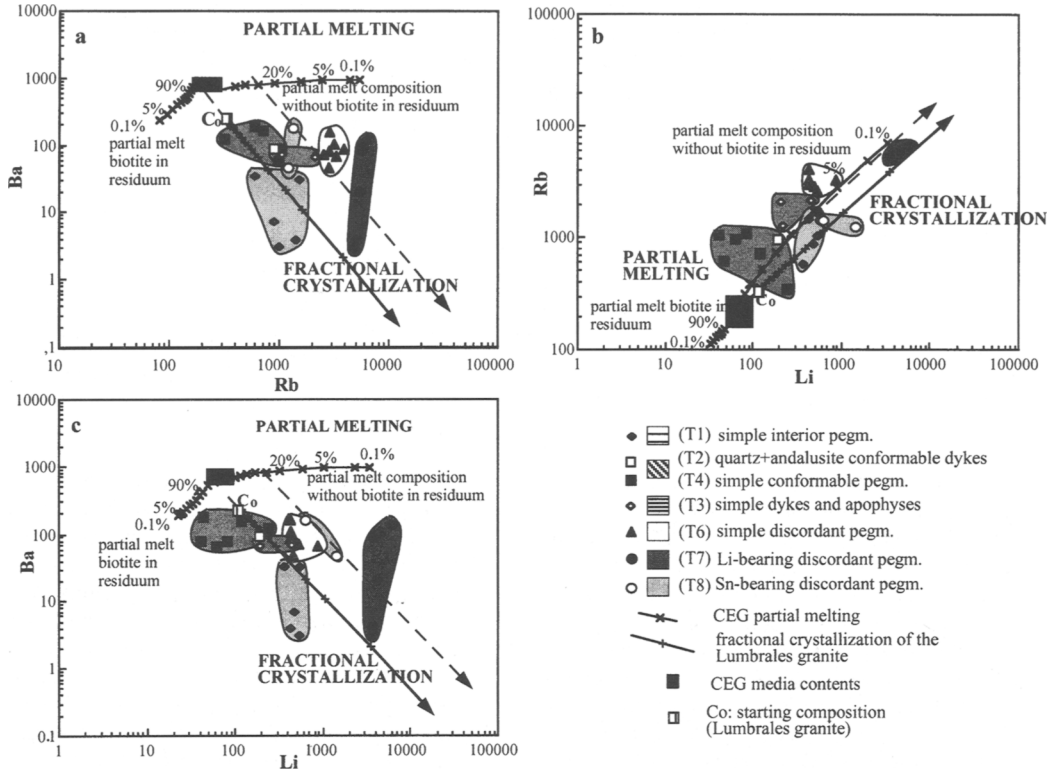

FIG. 8. Plot of (*a*) Ba *vs* Rb, (*b*) Rb *vs* Li and (*c*) Ba *vs* Li for the different pegmatite types, and the possible paths of fractional crystallization. Also illustrated are the paths of compositions of the melts which originated through partial melting, with and without biotite in the residuum.

melts capable of producing exotic granitic melts. These granitic melts could then crystallize following a fractional or an equilibrium crystallization, generating the most evolved granitic magmas.

Discussion

Field, mineralogical and petrographic criteria reveal that the pegmatites from the Fregeneda area show similar characteristics to many *REE* pegmatite fields.

(1) Paragenetic and geochemical features become more complex as one moves away from the Lumbrales granite (Fig. 1). Barren pegmatites crop out within (T1) or near to the granite (T2, T3, T4 and T5), whereas the pegmatites containing the highest concentrations of Li, Rb, Cs and/or Sn (T7 and T8) appear in the outermost zone. T6 pegmatites are between the barren and the most evolved ones, with an intermediate degree of fractionation.

(2) The most evolved pegmatites are less abundant than the barren ones, as proposed by Černý (1992).

(3) The barren pegmatites (T2, T3 and T4) are associated with the andalusite-sillimanite zones, whereas the more differentiated types (T5, T6, T7 and T8) appear in the biotite and chlorite zones of the regional metamorphism (Fig. 1). This means that the zoning tends to progress from barren pegmatites in higher-grade rocks toward the more fractionated pegmatites in lower-grade rocks.

(4) Some minerals are restricted to specific pegmatite types, e.g.: (a) the andalusite is restricted to pegmatites T2 and T4. It appears in pegmatites in low pressure metamorphic terrains, generally in the rare-element pegmatite formations. It usually appears only in the less evolved members of the pegmatitic sequence, as it occurs

in the Fregeneda area. (b) The occurrence of the main Fe-Mn phosphate association in the T6 pegmatites, between the barren and the more evolved dykes is in agreement with the pegmatite fields zonation established by Černý (1991). (c) Li-bearing mica is restricted to the T7 pegmatites, which crop out furthest from the Lumbrales granite. (d) Cassiterite is generally restricted to the more evolved zones, T7 and mainly in T8 dykes.

(5) Zoning is reflected not only in the mineral paragenesis of pegmatites, but also in the chemical composition of their main minerals: (a) the K/Rb ratio of micas and K-feldspar (Tables 3, 4; Figs 4, 5) (Roda *et al.*, 1995*a*) generally decreases with increasing fractionation, whereas the Li, Rb and Cs contents increase, in agreement with observations by other authors (Černý, 1992; Jolliff *et al.*, 1992; Shearer *et al.*, 1992, Mulja *et al.*, 1995; Neiva, 1995; Kontak and Martin, 1997). (b) Tourmaline changes composition with increasing distance from the Lumbrales granite. Thus, there is an overall increase of the Fe/Mg ratio parallel to the distance from the granite. (c) The Fe/(Fe+Mn) ratio is higher in phosphates associated with T6 pegmatites than in those associated with the Li-bearing T7 pegmatites, which is the normal trend shown by Fe-Mn phosphates during differentiation. Moreover, differences in the F content of montebrasite are apparent between the T6 and T7 pegmatites; it is richer in the Li-bearing pegmatites T7.

All these data suggest that the pegmatites from the Fregeneda area are the result of the same petrogenetic process. The plot of K/Rb *vs* Rb is significant for mica and K-feldspar (Fig. 5), as this plot shows the same trend for all members of a petrogenetic sequence (Dupuy and Allegre, 1972). All the pegmatite types of the Fregeneda area could be produced by a single process of magmatic evolution. Moreover, pegmatite spatial distribution fits well with the plot of the chemical composition of their minerals (Figs 1, 5). However, some data for the T8 pegmatites raise doubts about a single evolutionary trend. Firstly, these pegmatites are folded and in some cases are cut by the Li-bearing T7 pegmatites, whereas according to the zoning established by Černý (1991), the paragenesis of the T8 dykes (quartz, albite, muscovite and cassiterite) is typical of the last-forming members of a pegmatite sequence. Secondly, the K/Rb ratio of K-feldspar and micas associated with these dykes shows intermediate values (Tables 3, 4; Figs 4, 5), similar to those from the intragranitic T1 pegmatites. The Ba and Sr contents in mica and K-feldspar are also greater than expected in the last zone of a pegmatite sequence (Tables 3, 4). Thus, in columbite-tantalite from T8 dykes, the Nb and Fe contents are greater, and the Ta and Mn contents are less than in columbite-tantalite from the T4 and T7 pegmatites (Table 6). On the contrary, in a normal sequence of pegmatite evolution, the most evolved zones should have higher Mn and Ta and lower Fe and Nb contents (Černý *et al.*, 1985; Ercit, 1994; Suwimonprecha *et al.*, 1995; Mulja *et al.*, 1996; Wang *et al.*, 1997). Finally, the plot of the Rb, Li and Ba contents from the different pegmatite types, as well as the possible fractional crystallization paths from which such pegmatites would have originated, prove that not all the pegmatite types can be explained by a single crystallization path (Fig. 8).

Metapelitic and metaturbiditic series have generally been considered to be the main protolith of the rare element pegmatite fields because of their relative rare element enrichment. Vielzeuf and Holloway (1988) demonstrated that the melting of metapelites produces peraluminous melts, even without fluids. Nevertheless, the melting of a pelitic rock of typical composition, having biotite as a main constituent, would give rise to melts which do not have a low K/Rb ratio, high Li and Rb contents and low Ba values (Pearce *et al.*, 1984; Harris *et al.*, 1986), characteristics shown by the Lumbrales granite. Walker *et al.* (1989) showed the influence of mineral modes of the residues resulting from partial melting. Thus, the most suitable composition for generating alkali-rich melts would be a quartzo-feldspathic source rock, with a low biotite content.

Studies on the genesis of the Lumbrales granite are numerous. In general, all agree on an anatectic origin for the peraluminous Lumbrales and Saucelle leucogranites (Ugidos and Bea, 1976; Bea and Ugidos, 1976). Although the nature of the source rock has not yet been established, metagreywackes and quartzo-feldspathic gneisses of the schist-metagreywacke complex seem to be the most likely protoliths (Ugidos, 1988). The genesis of the Fregeneda pegmatites involves at least three different paths of fractional crystallization of melts generated by the partial melting of a quartz-feldspathic rock, with a composition similar to those of the CEG (Fig. 8). The path

corresponding to the highest melting degree (> 50%) fit with the evolution of a melt with a similar composition to that of the Lumbrales granite. The barren T1 and T3 pegmatites would have originated from this melt. The fractional crystallization of two melts originating from partial melting of <25% would give rise to the most evolved pegmatites: probably T6 and T7 on the one hand, and T8 on the other hand. The Sn-bearing T8 pegmatites would be earlier than the Li-bearing T7 pegmatites. The origin of the quartz-andalusite T2 dykes and the simple conformable T4 pegmatites seems to be related to the melt that was the source of the Lumbrales granite. Nevertheless, these bodies often show a lower degree of evolution than the granite, so they could be granitic and pegmatitic segregations earlier or contemporaneous with the genesis of such granite, as is described in other pegmatitic fields (Shearer *et al.*, 1987*b*, 1992). The K-feldspar T5 dykes might be included in the same crystallization path as the most evolved pegmatites, being generated prior to the T6 dykes. This assumption is based on field evidence (similar relationships to both the T6 and T7 bodies; and an outcrop area near the Lumbrales granite, but in the same zone as the T6 pegmatites); as well as on the geochemical data (plot of their K/Rb *vs* Rb for the K-feldspar, that put the T5 pegmatites in the same crystallization path as the most evolved pegmatites, but with a lower degree of differentiation) (Fig. 5). This model explains, on the one hand, the genesis of the Lumbrales granite and the pegmatites; and on the other hand, the plot of the K/Rb *vs* Rb values for micas and K-feldspar in a fractional crystallization model (Fig. 5).

Concluding remarks

(1) In the Fregeneda area, a rare-element pegmatite field occurs which shows enrichment in Li, Sn, Rb, Nb>Ta, B and P, and a regional zoning of different types of pegmatites is observed northwards from the Lumbrales granite. The following spatial sequence of pegmatite types can be observed from the granite outwards: (a) barren pegmatites (pegmatites T1, T2, T3 and T4) with a K, Al, Si, Na, B and P enrichment; (b) intermediate pegmatites (types T5 and T6), with a K, Na, Al, Si, P and Li enrichment; and (c) evolved pegmatites (dykes T7 and T8), with a Li, Sn, Nb>Ta, P and Rb enrichment.

(2) K-feldspar, micas and tourmaline are good indicators for setting up the petrogenetic relationships among pegmatites from a given pegmatite field, such as those of the Fregeneda pegmatites. High values of the K/Rb ratio occur in the barren T2 and T4 pegmatites, whereas lower values are characteristic of the more evolved T6 and T7 pegmatites. There is a zone with intermediate K/Rb values, where the T1, T3 and T5 pegmatite types overlap. The concentrations of lithophile elements, such as Li and Rb increase with the pegmatite evolution.

(3) The origin of the different pegmatite categories may account for three different paths of fractional crystallization of melts generated by the partial melting of a quartz-feldspathic rock, with a similar composition to that of the CEG (Fig. 8). The fractional crystallization of a melt formed by high degrees of partial melting (>50%) would give rise to the Lumbrales granite, the intragranitic T1 pegmatites, and the apophyses with aplitic and T3 pegmatitic facies. The T5 K-feldspar dykes, the simple discordant T6 pegmatites, the T7 Li-bearing pegmatites and also the T8 Sn-bearing dykes would have originated from the fractional crystallization of melts generated by lower degrees of partial melting. Finally, the quartz-andalusite T2 dykes, and the simple conformable T4 pegmatites, form pegmatitic segregations, earlier than, or at the same time as, the formation of the Lumbrales granite.

(4) Although this model explains the formation of all the pegmatite population cropping out in the Fregeneda area, the influence of other processes cannot be rejected. Partial melting of an heterogeneous source, or equilibrium crystallization intervals, alternating with fractional crystallization, may lead to a similar distribution and characteristics to those showed in the Fregeneda pegmatitic field.

Acknowledgements

The authors gratefully acknowledge the financial support of the Education, Universities and Investigation Department of the Basque Country Government. We also thank Dr A.M.R. Neiva for her suggestions and her critical review.

References

Ahrens, L.H., Pinson, W.H. and Kearnsand M.M. (1952) Association of rubidium and potassium and their

abundances in igneous rocks and meteorites. *Geochim. Cosmochim. Acta*, **2**, 229–42.

Appleman, D.E. and Evans, H.T. Jr. (1973) U. S. Geol. Surv., Comp. Contrib. 20, *U. S. Nat. Tech. Inf. Serv. Doc.*, PB2–16188.

Bathia, M.R. and Crooks, K.A.W. (1986) Trace element characteristics of graywackes and tectonic setting discrimination of sedimentary basins. *Contrib. Mineral. Petrol.*, **92**, 181–93.

Bea, F. (1976) Anomalía geoquímica de los granitoides calcoalcalinos hercínicos del área Cáceres-Salamanca-Zamora (España). Implicaciones petrogenéticas. *Stvd. Geol.*, **11**, 25–73.

Bea, F. and Ugidos, J.M. (1976) Anatexia inducida: petrogénesis de los granitos hespéricos de tendencia alcalina. Part I: leucogranitos del área O de Zamora y Salamanca. *Stvd. Geol.*, **11**, 9–24.

Bea, F., Sánchez, J.G. and Serrano Pinto, M. (1988) Una compilación geoquímica para los granitoides del macizo Hespérico. In *Geología de los granitoides y rocas asociadas del macizo Hespérico*. Rueda, Madrid, 87–192.

Beus, A.A. (1960) Geochemistry of beryllium and the genetic types of beryllium deposits. *Academy of Sciences of the USSR, Moscow*, 329 pp. (in Russian).

Borg, I.Y. and Smith, D.K. (1969) Calculated powder patterns. *Geol. Soc. Amer., Mem.*, **122**.

Carnicero, M.A. (1981) Granitoides del Centro Oeste de la Provincia de Salamanca. Clasificación y correlación. *Cuad. Lab. Xeol. Laxe*, **2**, 45–9.

Carnicero, M.A. (1982) Estudio del metamorfismo existente en torno al granito de Lumbrales (Salamanca). *Stvd. Geol.*, **17**, 7–20.

Černý, P. (1989) Characteristics of pegmatite deposits of tantalum. In *Lanthanides, Tantalum and Niobium* (P. Moller, P. Černý and F. Saupé eds). Springer Verlag, Berlin, Heidelberg, pp 195–239.

Černý, P. (1991) Rare-element granitic pegmatites. Part II: Regional to global environments and petrogenesis. *Geos. Can.*, **18**, 68–81.

Černý, P. (1992) Geochemical and petrogenetic features of mineralization in rare-element granitic pegmatites in the light of current research. *Appl. Geochem.*, **7**, 393–416.

Černý, P. and Hawthorne, F.C. (1982) Selected peraluminous minerals. In *Granitic Pegmatites in Science and Industry* (P. Černý, ed.). Mineral Assoc. Can., Short Course Handbook, **8**, 163–86.

Černý, P. and Meintzer, R.E. (1988) Fertile granites in the Archean and Proterozoic fields of rare-element pegmatites: crustal environment, geochemistry and petrogenetic relationships. In *Recent advances in the Geology of Granite-Related Mineral Deposits* (R.P. Taylor and D.F. Strong, eds). Canad. Inst. Min. Metall., Spec. Publ., **39**, 170–206.

Černý, P., Meintzer, R.E. and Anderson, A.J. (1985) Extreme fractionation in rare-element granitic pegmatites: selected examples of data and mechanisms. *Canad. Mineral.*, **23**, 381–421.

Dupuy, C. and Allegre, C.J. (1972) Fractionement K/Rb dans les suites ignimbritiques de Toscane. Un example de rejuvénation crustal. *Geochim. Cosmochim. Acta*, **36**, 437–58.

Ercit, T.S. (1994) The geochemistry and crystal chemistry of columbite-group minerals from granitic pegmatites, southwestern Grenville Province, Canadian Shield. *Canad. Mineral.*, **32**, 421–38.

García de Figuerola, L.C. and Parga, J.R. (1971) Características fundamentales de los 'sierros' de la provincia de Salamanca. *Bol. Geol. Min.*, **82-3-4**, 287–90.

García Garzón, J. and Locutura, J. (1981) Datación por el método Rb-Sr de los granitos de Lumbrales-Sobradillo y Villar de Ciervo-Puerto Seguro. *Bol. Geol. Min.* **92-1**, 68–72.

Goldschmidt, J.R. and Laves, F. (1954) The microcline-sanidine stability relations. *Geochim. Cosmochim. Acta*, **5**, 1–19.

Gonzalo Corral, J.C. (1981) *Estudio geológico del campo filoniano de La Fregeneda (Salamanca)*. Lic. Thesis. Univ. Salamanca, 77 pp.

Gromet, L.P., Dymek, R.F., Haskin, L.A. and Korotev, R.L. (1984) The North American shale composite: its compilation, major and trace element characteristics. *Geochim. Cosmochim. Acta*, **48**. 2469–82.

Harris, N.E.W., Pearce, J.A. and Tindle, A.G. (1986) Geochemical characteristics of collision-zone magmatism. In *Collision Tectonics* (M.P. Coward and A.C. Ries, eds). Blackwell Sci. Publ., Oxford., 67–81.

Hedge, C.E. (1966) Variations in radiogenic Strontium found in volcanic rocks. *J. Geophys. Res.*, **71**, 6119–26.

Heier, K.S. and Adams, J.A.S. (1964) The geochemistry of alkali metals. *Phys. Chem. Earth*, **5**, 255–380.

Hovis, G.L. (1986) Behavior of alkali feldspars: crystallographic properties and characterization of composition and Al-Si distribution. *Amer. Mineral.*, **71**, 869–90.

Jahns, R.H. and Burham, C.W. (1969) Experimental studies of pegmatite petrogenesis: I. A model for the derivation and crystallization of granitic pegmatites. *Econ. Geol.*, **64**, 843–63.

Jolliff, B.L., Papike, J.J. and Shearer, C.K. (1986) Tourmaline as a recorder of pegmatite evolution: Bob Ingersoll pegmatite, Black Hills, South Dakota. *Amer. Mineral.*, **71**, 472–500.

Jolliff, B.L., Papike, J.J. and Shearer, C.K. (1987) Fractionation trends in mica and tourmaline as indicators of pegmatite internal evolution: Bob Ingersoll pegmatite, Black Hills, South Dakota. *Geochim. Cosmochim. Acta*, **51**, 519–43.

Jolliff, B.L., Papike, J.J. and Shearer, C.K. (1992) Petrogenetic relationships between pegmatite and granite based on geochemistry of muscovite in pegmatite wall zones, Black Hills, South Dakota, USA. *Geochim. Cosmochim. Acta*, **56**, 1915–39.

Kontak, D.J. and Martin, R.F. (1997) Alkali feldspar in the peraluminous South Mountain Batholith, Nova Scotia: Trace-element data. *Canad. Mineral.*, **35**, 959–77.

Kroll, H. and Ribbe, P.H. (1983) Lattice parameters, composition and Al, Si order in alkali feldspars. In *Feldspar Mineralogy, 2nd edition*. Min. Soc. Amer., *Rev. Mineral.*, **2**, 57–99.

Kroll, H. and Ribbe, P.H. (1987) Determining (Al, Si) distribution and strain in alkali feldspars using lattice parameters and diffraction-peak positions: A review. *Amer. Mineral.*, **71**, 1–16.

London, D. (1992) The application of experimental petrology to the genesis and crystallization of granitic pegmatites. *Canad. Mineral.*, **30**, 499–540.

López Plaza, M. and Carnicero, M.A. (1988) El plutonismo Hercínico de la penillanura salmantino-zamorana (centro-oeste de España): Visión de conjunto en el contexto geológico regional. In *Geología de los granitoides y rocas asociadas del macizo Hespérico*. Rueda, Madrid, 53–68.

López Plaza, M. and Martínez Catalán, J.R. (1988) Síntesis estructural de los granitoides Hercínicos del macizo Hespérico. In *Geología de los granitoides y rocas asociadas del macizo Hespérico*. Rueda, Madrid, 195–210.

López Plaza, M., Carnicero, A. and Gonzalo, J.C. (1982) Estudio geológico del campo filoniano de La Fregeneda (Salamanca). *Stvd. Geol.*, **17**, 89–98.

Lottermoser, B.G. and Lu, J. (1997) Petrogenesis of rare-element pegmatites in the Olary Block, South Australia, part 1. Mineralogy and chemical evolution. *Mineral. Petrol.*, **59**, 1–19.

Martínez Fernandez, F.J. (1974) *Estudio del área metamórfica y granítica de los Arribes del Duero (Prov. de Salamanca y Zamora)*. Ph.D. Thesis, Univ. Salamanca, 286 pp.

Mata Burillo, F. (1986) *Geología del área granítico migmatítica de Lumbrales (Salamanca)*. Lic. Thesis. Univ. Salamanca, 72 pp.

Mulja, T., Williams-Jones, A.E., Martin, R.F. and Wood, S.A. (1995) Compositional variation and structural state of columbite-tantalite in rare-element granitic pegmatites of the Preissac-Lacorne batholith, Quebec, Canada. *Amer. Mineral.*, **81**, 146–57.

Mulja, T., Williams-Jones, A.E., Wood, S.A. and Boily, M. (1996) The rare-element-enriched monzogranite-pegmatite-quartz vein systems in the Preissac-Lacorne batholith, Quebec. I. Geology and Mineralogy. *Canad. Mineral.*, **33**, 793–815.

Neiva, A.M.R. (1995) Distribution of trace elements in feldspars of granitic aplites and pegmatites from Alijó-Sanfins, northern Portugal. *Mineral. Mag.*, **59**, 35–45.

Norton, J.J. (1981) Origin of lithium-rich pegmatitic magmas, southern Black Hills, South Dakota. *Geol. Soc. Amer., Abstr. Programs*, **34**, 221.

Norton, J.J. and Redden, J.A. (1990) Relations of zoned pegmatites to other pegmatites, granite, and metamorphic rocks in the southern Black Hills, South Dakota. *Amer. Mineral.*, **75**, 631–55.

Pearce, J.A., Harris, N.E.W. and Tindle, A.G. (1984) Trace element discrimination diagrams for the tectonic interpretation of granitic rocks. *J. Petrol.*, **25**, 956–83.

Roda, E. (1993) *Distribución, características y petrogénesis de las pegmatitas de La Fregeneda (Salamanca)*. Ph.D. Thesis, Basque Country Univ., 200 pp.

Roda, E., Pesquera, A. and Velasco, F. (1993) Mica and K-feldspar as indicators of pegmatite evolution in the Fregeneda area (Salamanca, Spain). In *Current Research in Geology Applied to Ore Deposits* (P. Fenoll Hach-Alí, J. Torres-Ruiz and F. Gervilla, eds), La Guioconda, Granada, 653–6.

Roda, E., Pesquera, A. and Velasco, F. (1995*a*) Micas of the muscovite-lepidolite series from the Fregeneda pegmatites (Salamanca, Spain). *Mineral. Petrol.* **55**, 145–57.

Roda, E., Pesquera, A. and Velasco, F. (1995*b*) Tourmaline in granitic pegmatites and their country rocks, Fregeneda area, Salamanca, Spain. *CanAD. Mineral.* **33**, 835–48.

Roda, E., Fontan, F., Pesquera, A. and Velasco, F. (1996) The phosphate mineral association of the granitic pegmatites of the Fregeneda area (Salamanca, Spain). *Mineral. Mag.*, **60**, 767–78.

Shearer, C.K., Papike, J.J. and Laul, J.C. (1985) Chemistry of potassium feldspars from three zoned pegmatites, Black Hills, South Dakota: Implications concerning pegmatite evolution. *Geochim. Cosmochim. Acta*, **49**, 663–73.

Shearer, C.K., Papike, J.J. and Laul, J.C. (1987*a*) Mineralogical and chemical evolution of a rare-element granite-pegmatite system: Harney Peak Granite, Black Hills, South Dakota. *Geochim. Cosmochim. Acta*, **51**. 473–86.

Shearer, C.K., Papike, J.J., Redden, J.A., Simons, S.B., Walker, R.J. and Laul, J.C. (1987*b*) Origin of pegmatitic granite segregetions, Willow Creek, Black Hills, South Dakota. *Canad. Mineral.*, **25**, 159–71.

Shearer, C.K., Papike, J.J. and Jolliff, B.L. (1992) Petrogenetic links among granites and pegmatites in the Harney peak rare-element granite-pegmatite system, Black Hills, South Dakota. *Canad. Mineral.*, **30**, 785–809.

Shmakin, B.M. (1979) Composition and structural state of K-feldspars from some U. S. pegmatites. *Amer. Mineral.*, **64**, 49–56.

Shmakin, B.M. (1983) Geochemistry and origin of granitic pegmatites. *Geochem. Int.*, **20**, 1–8.

Sokolov, Yu.M. (1981) Precambrian metamorphogenic pegmatites. In *The Development Potential of Precambrian Mineral Deposits*. Nat. Resour. and Energy Div., U. N. Dept Tech. Co-op. for Development, Pergamon, 157–64.

Stewart, D.B. (1978) Petrogenesis of lithium-rich pegmatites. *Amer. Mineral.*, **63**, 970–80.

Suwimonprecha, P., Černý, P. and Friedrich, G. (1995) Rare metal mineralization related to granites and pegmatites, Phuket, Thailand. *Econ. Geology*, **90**, 603–15.

Ugidos, J.M. (1988) Asimilación en los granitos hercínicos: aspectos básicos e implicaciones. In *Geología de los granitoides y rocas asociadas del macizo Hespérico* Rueda, Madrid., 315–20.

Ugidos, J.M. and Bea, F. (1976) Análisis comparativo de los granitos del área Béjar-Plasencia con otros granitos 'younger' centro peninsulares: precisiones sobre la serie mixta. *Stvd. Geol.*, **10**, 45–59.

Vielzeuf, D. and Holloway, J.R. (1988) Experimental determination of the fluid-absent melting relations in the pelitic system. *Contrib. Mineral. Petrol.*, **98**, 257–76.

Walker, R.J., Hanson, G.N. and Papike, J.J. (1989) Trace element constraints on pegmatite genesis: Tin Mountain pegmatite, Black Hills, South Dakota. *Contrib. Mineral. Petrol.*, **101**, 290–300.

Wang, R.Ch., Fontan, F., Xu, S.J., Chen, X.M. and Monchoux, P. (1997) The association of columbite, tantalite and tapiolite in the Suzhou granite, China. *Canad. Mineral.*, **35**, 699–706.

Wright, T.L. and Stewart, D.B. (1968) X-ray and optical study of alkali feldspar: I Determination of composition and structural state from refined unit cell parameters and 2V. *Amer. Mineral.*, **53**, 38–87.

[*Manuscript received 21 May 1998: revised 13 November 1998*]